Journal of Nuclear Materials 384 (2009) 109–114

Contents lists available at ScienceDirect

Journal of Nuclear Materials

journal homepage: www.elsevier.com/locate/jnucmat

The effect of copper and manganese on magnetic minor hysteresis loops in neutron irradiated Fe model alloys

S. Kobayashi [a,*], H. Kikuchi [a], S. Takahashi [a], Y. Kamada [a], K. Ara [a], T. Yamamoto [b], D. Klingensmith [b], G.R. Odette [b]

[a] NDE and Science Research Center, Faculty of Engineering, Iwate University, Morioka 020-8551, Japan
[b] Department of Mechanical and Environmental Engineering, University of California Santa Barbara, Santa Barbara, CA 93106, USA

ARTICLE INFO

Article history:
Received 17 December 2007
Accepted 15 October 2008

PACS:
61.80.Hg
75.60.Ej
75.50.Bb
61.72.−y

ABSTRACT

Changes of magnetic minor hysteresis loops in pure Fe, Fe–1 wt% Mn, Fe–0.9 wt% Cu, and Fe–0.9 wt% Cu–1 wt% Mn model alloys after neutron irradiation have been studied. Minor-loop coefficients which are obtained from scaling relations between minor-loop parameters and in proportion to internal stress, were found to decrease in all model alloys after the irradiation to a fluence of 3.32×10^{19} n cm^{-2}. The decrease of the coefficients is larger for alloys including Cu and is enhanced by 1 wt% Mn addition. Such decrease implying the reduction of internal stress during irradiation is in contrast with changes of yield strength after the irradiation that increase with Cu and Mn contents. A qualitative explanation was given on the basis of the preferential formation of Cu precipitates along pre-existing dislocations which reduces internal stress of the dislocations.

1. Introduction

Accurate evaluation of neutron irradiation embrittlement of nuclear reactor pressure vessel steels and prediction of their lifetime have a key role for integrity assessments of nuclear reactors during operation. Long-term irradiation with high-energy neutrons makes ductility of steels lower and susceptible to rupture [1–3]. Irradiation embrittlement is associated with changes in various mechanical properties such as an increase in ductile–brittle transition temperature (DBTT), hardness, yield strength as well as a decrease in upper shelf energy. Currently, the irradiation embrittlement of pressure vessels is characterized by a change of DBTT obtained by Charpy impact tests, which is a destructive testing. However, the diminishing stock of Charpy specimens preinstalled in the reactors has became an urgent problem for long-term operation of nuclear reactors beyond their designed lifetime. An establishment and practical realization of a reliable non-destructive testing method are required [4].

The mechanisms of irradiation embrittlement related to the material hardening have been extensively investigated with various experimental methods ranging from fundamental bulk measurements such as DBTT, yield strength, microhardness, electrical resistivity, Seebeck coefficient, to direct nanoscale measurements such as transmission electron microscopy, atom-probe tomography, small-angle neutron scattering, positron annihilation [1,3]. It has been shown that the hardening is primarily due to the formation of nanoscale defects such as Cu rich precipitates, dislocation loops, solute-vacancy clusters etc., which pin dislocations from movement [2,3]. The nucleation and growing processes of these defects during neutron irradiation was found to be strongly influenced by various factors including neutron flux, irradiation temperature, chemical composition, and heat treatment prior to irradiation [3,5,6].

The magnetic method using hysteresis loops is one of useful non-destructive methods to get information on lattice defects [7–18]. Since magnetic domain walls interact with lattice defects through magnetostatic, magnetoelastic couplings etc., their movement is largely disturbed by the defects. The effective strength of the interactions depends on the size, density, spatial distribution, and kinds of lattice defects, which is reflected in a shape of magnetic hysteresis loops. It was revealed in cold-rolled steels [16] that coercive force H_c, which is one of important structure-sensitive hysteresis properties, is proportional to hardness and DBTT. Such good relationship between magnetic and mechanical properties has been confirmed in various steels where defect density is controlled by plastic deformation [9,13], thermally ageing [10,11], pre-heat treatment [12], and chemical compositions [12].

In spite of the deep understanding of magnetic properties in these steels, however, results of magnetic properties in neutron irradiated steels are still controversial [4,19–26]. For instance, in A533B nuclear pressure vessel steels irradiated to the fluence of about 1×10^{19} n cm^{-2}, H_c was found to decrease after neutron irradiation [21–23], whereas some groups reported the increase or no

* Corresponding author. Tel./fax: +81 19 621 6350.
E-mail address: koba@iwate-u.ac.jp (S. Kobayashi).

0022-3115/$ - see front matter © 2008 Elsevier B.V. All rights reserved.
doi:10.1016/j.jnucmat.2008.10.031

significant changes [19,20]. This discrepancy is mainly attributed to a slight difference in an experimental set-up as well as sample conditions including pre-heat treatment, chemical compositions. Systematic investigation of magnetic property changes and construction of their database are indispensable for the practical realization of the magnetic method for nondestructive evaluation of pressure vessels.

Quite recently, we performed measurements of a set of minor hysteresis loops in neutron-irradiated Fe–Cu–Ni–Mn model alloys, where chemical compositions of Cu (0.05–0.9 wt%) and Ni (0.8, 1.6 wt%) contents were systematically varied [18]. It was found that minor-loop coefficients which are in proportion to internal stress decrease after neutron irradiation to a fluence of 0.44×10^{19} n cm^{-2} for all alloys. The decrease of the coefficients strongly depends on both Cu and Ni contents and is enhanced for high-Cu high-Ni alloy. Further, the decrease of the coefficients is roughly in inverse proportion to changes of yield strength.

In this paper, we focused on changes of magnetic minor hysteresis loops in neutron-irradiated pure Fe, Fe–1 wt% Mn, Fe–0.9 wt% Cu, and Fe–0.9 wt% Cu–1 wt% Mn model alloys with no Ni inclusion. The compositions are more fundamental compared with those of previous Fe–Cu–Ni–Mn model alloys, but the obtained results would give a deep insight into roles of each irradiation defect on minor-loop properties. The results were explained from the viewpoint of nanoscale features of irradiation defects which were revealed by atom-probe tomography, small-angle neutron scattering, positron annihilation using the same materials [27–29].

2. Experimental

We examined four model alloys listed in Table 1; Fe (VA), Fe–1.0 wt% Mn (VB), Fe–0.9 wt% Cu–1.0 wt% Mn (VD), and Fe–0.9 wt% Cu (VH) alloys. The alloys were solution treated for 17 h at 775 °C and then salt-bath quenched at 450 °C for 3 min, followed by slow cooling to room temperature in air.

Tensile test samples in the form of 24 mm × 5 mm × 0.5 mm coupon were neutron irradiated at the University of Michigan Ford Nuclear Reactor under the University of California, Santa Barbara (UCSB) irradiation variable (IVAR) program. The irradiation condition is listed in Table 2. The maximum fluence ϕt was 3.32×10^{19} n cm^{-2} and the neutron flux ϕ was 0.77 or 0.97×10^{12} n cm^{-2} s^{-1}, which is categorized as high flux regime [6]. We examined the T6 condition for all model alloys, and also the K2 condition for the VD alloy. The irradiation temperature was 290 °C.

Magnetic hysteresis measurements were performed at room temperature using an apparatus designed for neutron-irradiated tensile test samples [18]. The sample was fixed by upper and lower yokes made of Fe–3 wt% Si steel, which forms a closed magnetic circuit. A cyclic magnetic field with a frequency of 1 Hz was applied along the long axis of the sample, by an exciting coil wound around the sample. The details of the measurement system is given in Ref. [18].

A set of quasistatic magnetic minor hysteresis loops with various amplitude of a cyclic field, H_a up to 6 kA/m, was measured by increasing H_a, step by step. Before measuring each minor loop, the sample was demagnetized with decaying alternating magnetic field and then a minor loop, which is symmetric about the origin, was measured. These minor loops are different from the major loop, obtained with H_a large enough for saturation. In the present study, the hysteresis loop with H_a = 6 kA/m was assumed to be the major loop. The magnetic properties for each alloy-irradiation condition were obtained from 1 or 2 samples. For our measurement system, an experimental accuracy of magnetic properties was within 1 % for each sample and errors of magnetic properties are mainly due to their sample dependence.

Our analysis [14–16] showed that there exist several simple relations between parameters of minor loops in a limited range of H_a:

$$W_F^* = W_F^0 \left(\frac{M_a^*}{M_s}\right)^{n_F}, \quad (1)$$

$$W_R^* = W_R^0 \left(\frac{M_R^*}{M_R}\right)^{n_R} \quad (2)$$

and

$$H_c^* = H_c^0 \left(\frac{M_R^*}{M_R}\right)^{n_c}. \quad (3)$$

Here, M_a^*, M_R^*, W_F^*, W_R^* and H_c^* are minor-loop magnetization, minor-loop remanence, minor-loop hysteresis loss, minor-loop remanence work, and minor-loop coercive force, respectively, as denoted in Fig. 1. M_s and M_R are saturation magnetization and remanence of the major loop, respectively. The relations of Eqs. (1)–(3) are valid for minor loops where irreversible movement of Bloch wall mainly contributes to magnetization. The exponents of the power laws, n_F, n_R, and n_c are nearly 1.5, 1.5, and 0.45, respectively, and are almost independent of kinds of materials. Note that the relation of Eq. (1) is known as Steinmetz law where $n_F \sim 1.6$ [30]. W_F^0, W_R^0, and H_c^0 are minor-loop coefficients independent of magnetic field and amplitude of a cyclic field. The coefficients are proportional to internal stress and more sensitive to it compared with H_c. In this study, these coefficients were used to investigate changes of internal stress in the model alloys after neutron irradiation.

3. Experimental results

To see changes of magnetic properties due to neutron irradiation, we first pay attention to major loops. Fig. 2(a)–(d) shows ma-

Table 1
Chemical compositions of measuring samples.

Sample	Cu (wt%)	Mn (wt%)	N (wt ppm)
VA			5
VB		1.0	40
VD	0.9	1.0	10
VH	0.9		20

Table 2
Neutron irradiation conditions in this study.

	Flux ϕ (10^{12} n cm^{-2} s^{-1})	Fluence ϕt (10^{19} n cm^{-2})
K2	0.77	0.55
T6	0.97	3.32

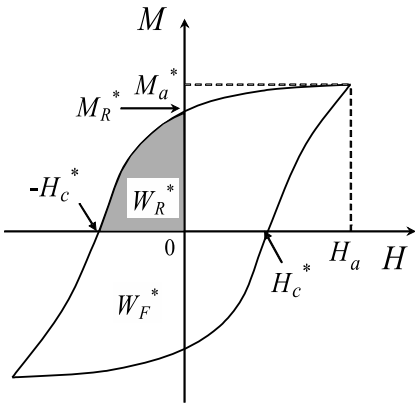

Fig. 1. Parameters of a minor loop.

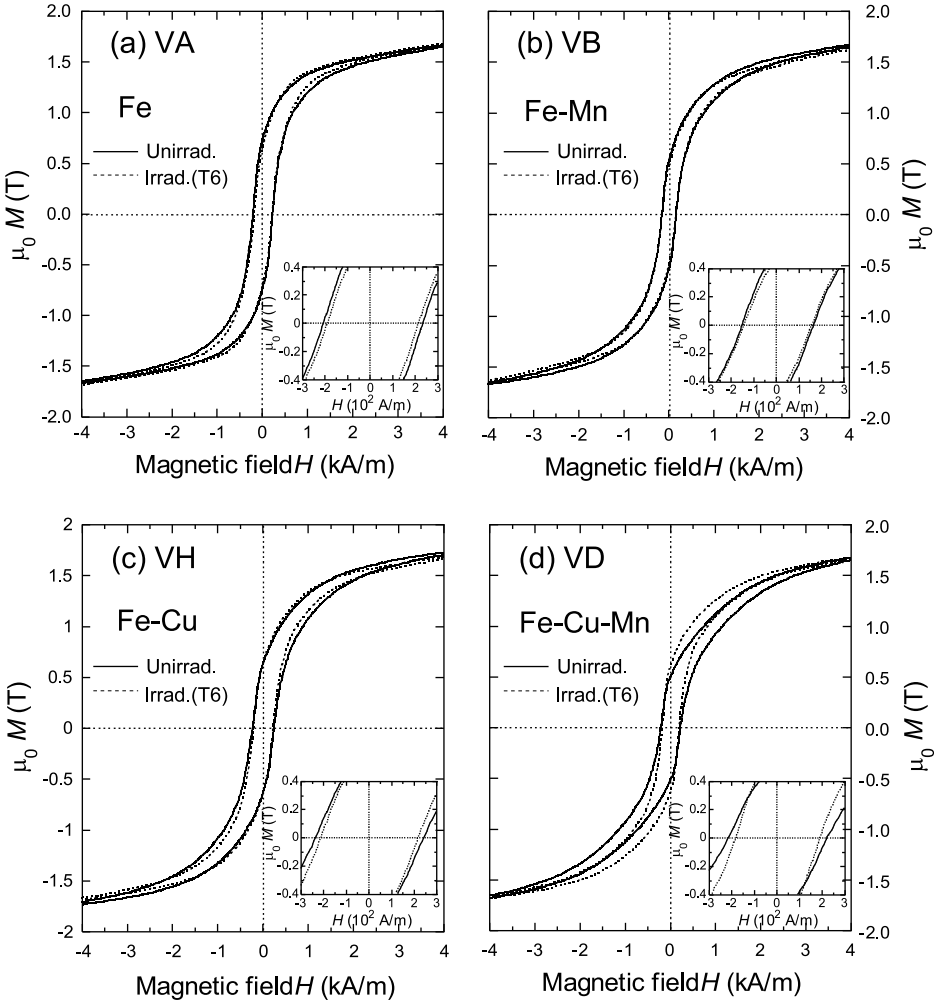

Fig. 2. Major loops for (a) VA, (b) VB, (c) VH, and (d) VD, before and after neutron irradiation in T6 condition. The solid and dashed lines show data for unirradiated and irradiated samples, respectively.

jor loops for VA, VB, VH, VD samples, respectively, before and after neutron irradiation in T6 condition. One can see that for both VA and VB samples a change of the major loop due to neutron irradiation is very small, whereas a significant increase of the slope of the sides of the major loop was observed for both VH and VD samples. As is seen in the inset in Fig. 2, the coercive force H_c at which the magnetization becomes zero decreases for all samples after the T6 irradiation and is most pronounced for VD alloy with high Cu and high Mn contents. These results indicate that both Cu and Mn atoms give a large influence on the magnetic properties.

To investigate the changes of magnetic properties in more detail, we measured a set of minor loops with various H_a and analyzed them according to Eqs. (1)–(3). Fig. 3 shows typical examples of set of minor loops, where the data for VH and VD alloys before and after T6 irradiation are shown. As was observed for the major loop, the slope of the loops at minor-loop coercive force where $\mu_0 M = 0$ becomes larger and the loop width becomes narrower after the irradiation for both alloys when minor loops measured with the same H_a are compared. Particularly, the smaller H_a, the larger the change of the minor loop. This shows the high sensitivity of minor loops to microstructural changes due to neutron irradiation.

Fig. 4 shows double logarithmic plots of the relation between W_F^* and M_a^* for VH and VD alloys before and after T6 irradiation. The $W_F^* - M_a^*$ curves show straight lines in a limited range of M_a^* and their slopes are almost the same for all alloy-irradiation condition. This M_a^* range corresponds to the field range where the irreversible displacement of Bloch wall plays a crucial role for magnetization and M_a^* has a steep slope in the H_a dependence [14–16]. Such a linear relation was also observed for double logarithmic plots of $W_R^* - M_R^*$ and $H_c^* - M_R^*$ curves.(not shown) From least-squares fits of the data to Eqs. (1)–(3), both exponents and minor-loop coefficients were determined. Here, minor loops with $\mu_0 M_a^*$ = 0.2–1.1 T were used for the fits and n_F = 1.67 ± 0.08, n_R = 1.59 ± 0.08, and n_c = 0.47 ± 0.04. Since all minor-loop coefficients W_F^0, W_R^0, and H_c^0 show a similar dependence on neutron fluence with each other, we will show only the data for W_F^0.

Fig. 5 shows W_F^0 as a function of neutron fluence ϕt. For all samples W_F^0 was found to decrease by neutron irradiation to $\phi t = 3.32 \times 10^{19}$ n cm^{-2}. The decrease for both VA and VB samples is almost the same with each other, indicating the Mn addition to pure Fe has little influence on W_F^0. On the other hand, adding Cu to pure Fe gives a significant influence on the decrease in W_F^0 as is seen for VH alloy. Such a large decrease in W_F^0 due to Cu inclusion was also observed in our previous magnetic measurements on Fe–Cu–Ni–Mn model alloys [18]. For VH alloy with both Cu and Mn contents, the decrease in W_F^0 due to irradiation is further enhanced. These results indicate the synergistic effect between Cu and Mn atoms on the decrease of W_F^0, i.e. the reduction of internal stress during neutron irradiation.

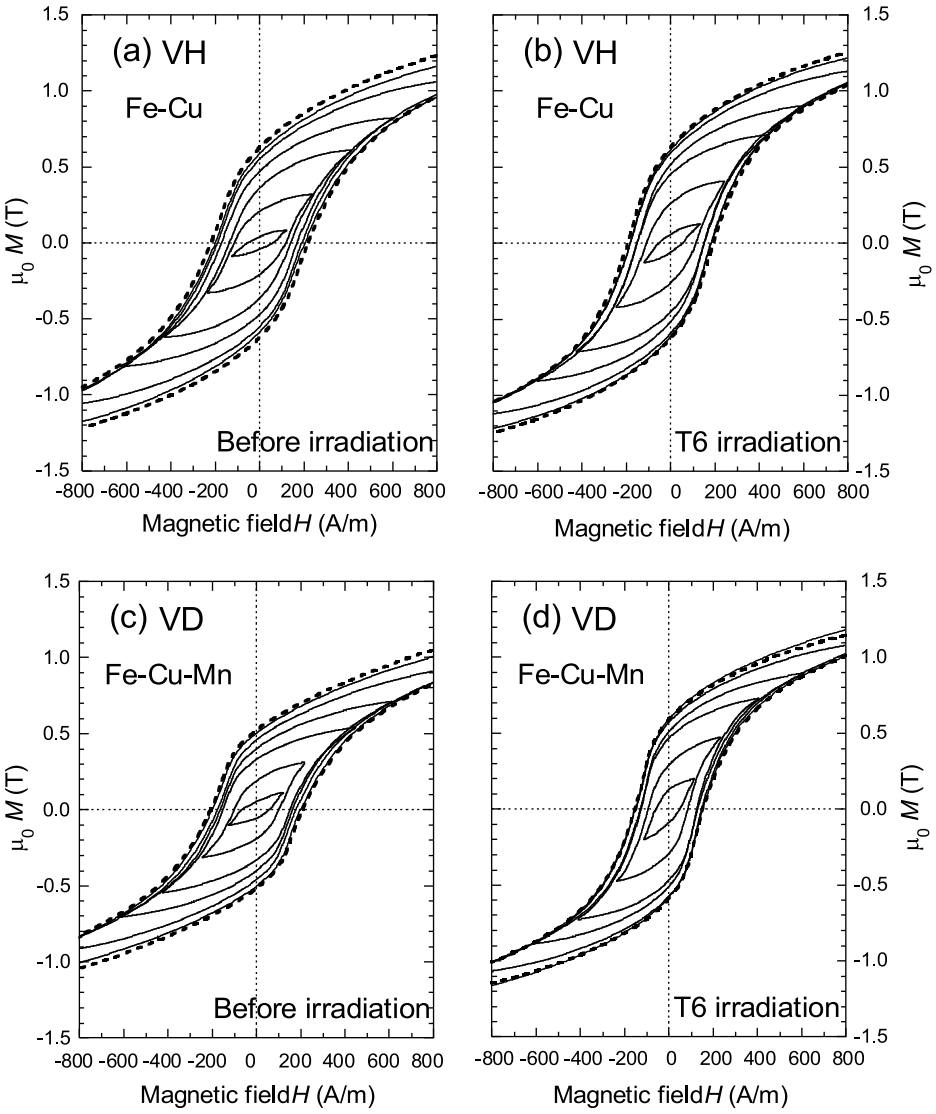

Fig. 3. Set of minor hysteresis loops for VH alloy (a) before and (b) after neutron irradiation in T6 condition, and for VD alloy (c) before and (d) after the irradiation. The solid and dotted lines represent minor loops and the major loop, respectively. For clarity, only representative loops are shown.

Note that W_F^0 for VD alloy seems to have a peak at low fluence of $\sim 0.5 \times 10^{19}$ n cm^{-2}, though the data include a large error due to the sample dependence. Such a peak was also observed in Fe–Cu–Ni–Mn model alloys [18] and A533B-typle reactor pressure vessel steels [17] at $\phi t \sim 0.05 \times 10^{19}$ and 1×10^{19} n cm^{-2}, respectively. The appearance of a peak and its position against fluence seem to depend on chemical compositions and the detailed investigation will appear elsewhere.

4. Discussion

Nanoscale features of lattice defects during neutron irradiation have been extensively investigated with various methods including transmission electron microscopy, small-angle neutron scattering, atom probe tomography, positron annihilation spectroscopy etc. It has been shown that neutron irradiation induces the formation of nanoscale defects such as Cu-rich precipitates, dislocation loops, solute clusters, solute-vacancy clusters, etc. These defects act as pinning center for dislocations and disturb their movement, resulting in changes of mechanical properties after irradiation; an increase of hardness, DBTT, yield strength as well as a decrease of ductility, upper shelf energy.

Fig. 6 shows a change of yield strength $\Delta\sigma_y$ after neutron irradiation to $\phi t = 3.32 \times 10^{19}$ n cm^{-2}.(T6 condition) The yield strength was determined by tensile tests performed by UCSB group. The tests were carried out for two or more samples for each alloy-irradiation condition. For both VA and VB alloys, $\Delta\sigma_y$ is about 50 MPa and is relatively small compared with that for VH and VD alloys. The increase of the yield strength for VA and VB alloys is mainly attributed to the formation of dislocation loops, though for VB alloy fine scale manganese-vacancy clusters in subnanometer size are considered to give additional effects [5,31].

The addition of copper largely increases $\Delta\sigma_y$ as is seen for VH and VD alloys in Fig. 6. This is primarily due to the nucleation and growth of a high number density of Cu precipitates. Such Cu precipitates are the dominant feature for the material hardening, when the material contains copper greater than about 0.1 wt% [3]. Previous atom probe tomography and small-angle neutron scattering studies for VH and VD alloys revealed that the number density and size of Cu precipitates for VH (Fe–Cu) alloy are about 7×10^{22} m^{-3} and about 2.8 nm, respectively, after neutron irradiation to the fluence of $\phi t \sim 1 \times 10^{19}$ n cm^{-2}. However, addition of 1 wt% Mn was found to greatly increase the number density and

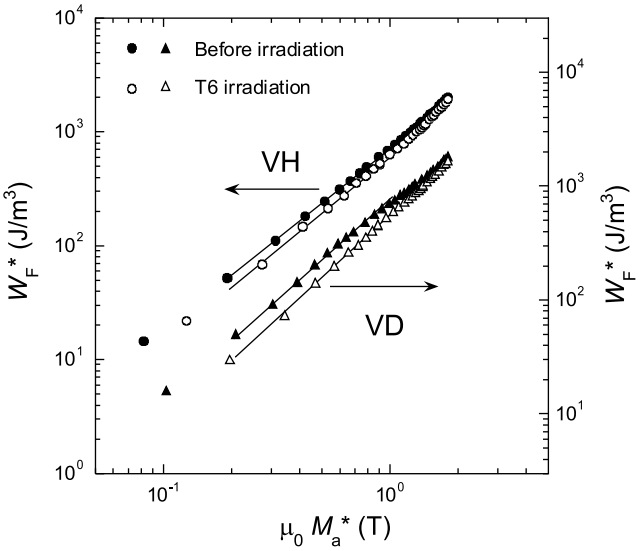

Fig. 4. Relations between W_F^* and M_a^* for VH (circles) and VD (triangles) alloys before and after neutron irradiation in T6 condition. The solid and open symbols denote the data before and after T6 irradiation, respectively. The solid lines through the data show least-squares fits.

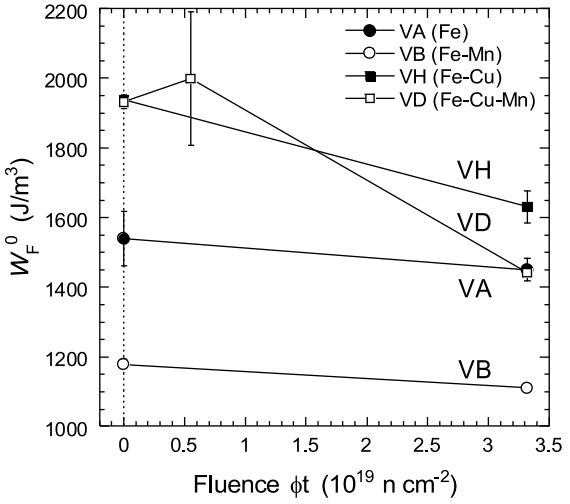

Fig. 5. W_F^0 as a function of neutron fluence; VA (solid circles), VB (open circles), VH (solid squares), and VD (open squares).

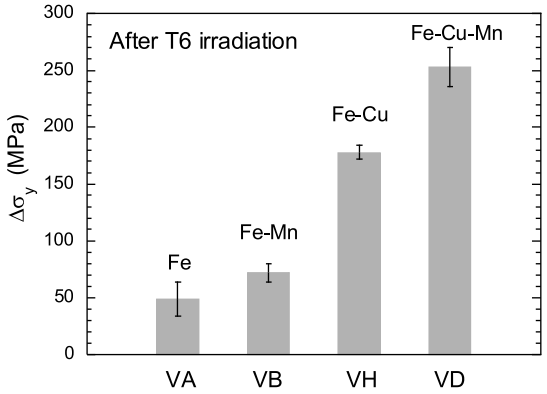

Fig. 6. A change in yield strength $\Delta\sigma_y$ after neutron irradiation in T6 condition.

reduce the size of Cu-rich precipitates in VD (Fe–Cu–Mn) alloy; 7 $\times 10^{23}$ m^{-3} in density and about 1.8 nm in size.

Depending on chemical compositions, various kinds of lattice defects are formed by neutron irradiation. These defects also interact with magnetic domain walls and influence their movement. According to an earlier theory for micromagnetism [7], the arrangement of magnetization is determined so as to minimize magnetic Gibbs free energy consisting of exchange energy, magnetocrystalline anisotropy energy, magnetostatic energy, and magnetoelastic energy. In ferromagnets including lattice defects, the Gibbs free energy is lowered when domain walls are located at lattice defects and the defects act as obstacles to the domain wall motion. Therefore, one will expect that the formation of irradiation defects results in an increase of minor-loop coefficients after neutron irradiation. However, the present study showed that the coefficients rather decrease during neutron irradiation and the decrease is remarkably enhanced for VD alloy with both Cu and Mn contents. The trend after irradiation is opposite to that of yield strength and a change of the minor-loop coefficient, ΔW_F^0, after T6 irradiation is roughly in inverse proportion to $\Delta\sigma_y$ as shown in Fig. 7. This indicates that the harder material mechanically, the softer the material magnetically.

This relationship which, at first glance, seems to be contradictory was also observed in Fe–Cu–Ni–Mn alloys [18] and would be explained by assuming the preferential formation of Cu precipitates along pre-existing dislocations besides the formation in the matrix [17,18,32,33]. Since both precipitates and dislocations include stress field, precipitates will be preferentially formed along dislocations to reduce the elastic energy. As a result, the internal stress will become lower around dislocations. If such reduction of internal stress has a significant influence on magnetic properties compared with the increase due to irradiation defects formed in the matrix, an observed minor-loop coefficient will decrease after neutron irradiation as was observed for VH and VD alloys in the present study. The internal stress around dislocations will be further reduced as the number density of precipitates increases. This might be responsible for the larger decrease of W_F^0 for VD alloy with the smaller size and higher number density of precipitates.

For VA and VB alloys with no Cu content, on the other hand, the increase of $\Delta\sigma_y$ and the decrease of ΔW_F^0 after the irradiation are drastically reduced. In these alloys, no precipitates were confirmed and instead, dislocation loops (also manganese-vacancy clusters for VB alloy) would play a crucial role for both mechanical and magnetic properties. From the viewpoints of the interaction between dislocation loops and pre-existing dislocations, it may be

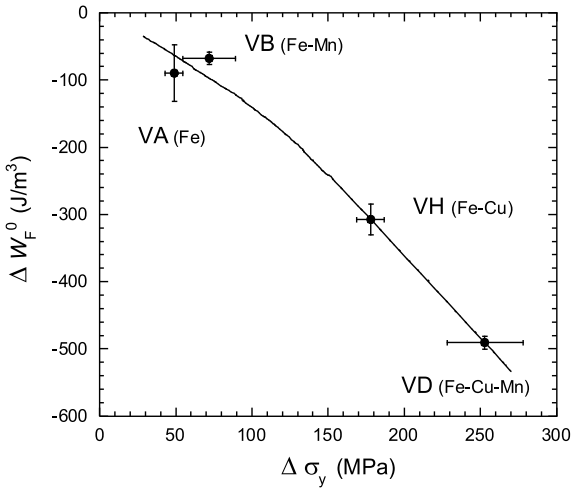

Fig. 7. Relation between a change in minor-loop coefficient ΔW_F^0 and a change in yield strength $\Delta\sigma_y$, after neutron irradiation to $\phi t = 3.32 \times 10^{19}$ n cm^{-2}.

possible to compensate the internal stress of pre-existing dislocations by dislocation loops formed around them as revealed by previous TEM observations on neutron irradiated pure iron [34,35] and reactor pressure vessel steels [36]. This reduces the internal stress of the dislocations, giving rise to the decrease of W_F^0 after the irradiation.

It should be noted that in previous in-situ magnetic measurements during neutron irradiation [17], a monotonic increase of W_F^0 with fluence was observed for pure Fe. However, H_c before irradiation is about 60 A/m and is much smaller than about 200 A/m for VA alloy. This means that for the previous pure Fe sample dislocation density is very low and dislocation loops formed in the matrix therefore exert a significant effect on W_F^0.

In this study, the decrease of W_F^0 after neutron irradiation was explained as due to the formation of precipitates or dislocation loops around pre-existing dislocations. These defects, on the one hand, pin the dislocations from movement and would make yield strength increase. Though effects of such pinning on mechanical properties, relative to those due to defects in the matrix, are not fully understood yet [32], the proposed irradiation mechanism based on the preferential formation of precipitates (or dislocation loops) is not in contradiction to the observed data of yield strength.

5. Conclusion

The effects of copper and manganese in neutron-irradiated pure Fe, Fe–1 wt% Mn, Fe–0.9 wt% Cu, and Fe–0.9 wt% Cu–1 wt% Mn model alloys were investigated by measurements of magnetic minor hysteresis loops. Minor-loop coefficients, which are a sensitive indicator of internal stress, were determined from scaling relations between field dependent minor-loop parameters. For all model alloys, the coefficients decrease after neutron irradiation to a fluence of 3.32×10^{19} n cm^{-2} and the decrease depends on chemical composition. The addition of 1 wt% Mn to pure Fe has no significant influence on the minor-loop properties, but the combination of 1 wt% Mn and 0.9 wt% Cu strongly enhances the decrease of coefficients. The decrease is larger than that for binary Fe–0.9 wt% Cu alloy, indicating the synergistic effect between Cu and Mn atoms. A possible mechanism that irradiation defects are preferentially formed along pre-existing dislocations was introduced to explain the results.

Changes of yield strength are generally a monotonically increasing function of neutron fluence and are a good indicator of material hardening. On the other hand, the behavior of magnetic properties during neutron irradiation is not simple and there exist two competing irradiation mechanisms that affect the properties; the formation of irradiation defects in the matrix and the preferential formation of irradiation defects around pre-existing dislocations. Which mechanism dominates the magnetic property changes seems to depend on the material's initial condition (density of pre-existing dislocations, microstructure etc.) as inferred from fluence dependence of minor-loop coefficients for pure iron. However, if the initial condition is almost the same, changes of magnetic properties due to neutron irradiation are well related with yield strength as demonstrated in the present study as well as previous works for Fe–Cu–Ni–Mn model alloys. This implies that the material hardening can be evaluated for any irradiated materials by magnetic method if the material's initial condition and its influence on the relation between changes of minor-loop properties and yield strength are known. Development of the database of the relation in various alloy-irradiation condition taking account of material's initial condition is now in progress and the results will appear elsewhere.

Acknowledgement

This research project has been conducted under the research contract with the Japan Nuclear Safety Organization (JNES).

References

[1] J. Koutský, J. Kočík, Radiation Damage of Structural Materials, Elsevier Science Publishers, 1994. and references therein.
[2] G.R. Odette, G.E. Lucas, JOM 53 (2001) 18.
[3] G.R. Odette, G.E. Lucas, Radiat. Eff. Def. Solids 144 (1998) 189. and references therein.
[4] M. Blaszkiewicz, Mater. Sci. Forum 210–213 (1996) 9.
[5] G.R. Odette, G.E. Lucas, D. Klingensmith, B.D. Wirth, D. Gragg, NUREG/CR-6778, US Nuclear Regulatory Commission, Washington, DC, 2003.
[6] G.R. Odette, T. Yamamoto, D. Klingensmith, Philos. Mag. 85 (2005) 779.
[7] H. Kronmüler, M. Fähnle, Micromagnetism and the Microstructure of Ferromagnetic Solids, Cambridge University, Cambridge, 2003.
[8] J.B. Goodenough, Phys. Rev. 95 (1954) 917.
[9] L.J. Dijkstra, C. Wert, Phys. Rev. 79 (1950) 979.
[10] L.P. Vandenbossche, M.J. Konstantinovic, A. Almazouzi, L.R. Dupre, J. Phys. D: Appl. Phys. 40 (2007) 4114.
[11] Y. Kamada, D.G. Park, S. Takahashi, H. Kikuchi, S. Kobayashi, K. Ara, J.H. Hong, I.G. Park, IEEE Trans. Mag. 43 (2007) 2701.
[12] D.C. Jiles, J. Phys. D: Appl. Phys. 21 (1988) 1186.
[13] D.C. Jiles, J. Phys. D: Appl. Phys. 21 (1988) 1196.
[14] S. Takahashi, L. Zhang, J. Phys. Soc. Jpn. 73 (2004) 1567.
[15] S. Takahashi, L. Zhang, S. Kobayashi, Y. Kamada, H. Kikuchi, K. Ara, J. Appl. Phys. 98 (2005) 033909/1-8.
[16] S. Takahashi, S. Kobayashi, H. Kikuchi, Y. Kamada, J. Appl. Phys. 100 (2006) 113908/1-6.
[17] S. Takahashi, H. Kikuchi, K. Ara, N. Ebine, Y. Kamada, S. Kobayashi, M. Suzuki, J. Appl. Phys. 100 (2006) 023902/1-6.
[18] S. Kobayashi, H. Kikuchi, S. Takahashi, K. Chiba, Y. Kamada, K. Ara, Philos. Mag. 87 (2007) 4047.
[19] J.F. Stubbins, W.J. Shong, M. Giacobbe, A.M. Ougouag, J.G. Williams, ASTM STP-1204 (1993) 5.
[20] M. Otaka, S. Shimizu, R. Morinaka, N. Maeda, A. Yamaguchi, ASTM STP-1325 (1999) 568.
[21] T. Goto, T. Kamimura, S. Kumano, I. Takeuchi, N. Maeda, A. Yamaguchi, ASTM STP-1325 (1999) 589.
[22] M.K. Devine, D.C. Jiles, P.K. Liaw, R.D. Rishel, D.S. Drinon, Rev. Prog. Quantitative NDE 12 (1993) 1815.
[23] L.B. Sipahi, M.R. Govindaraju, D.C. Jiles, J. Appl. Phys. 75 (1994) 6981.
[24] D.G. Park, C.G. Kim, H.C. Kim, J.H. Hong, I.S. Kim, J. Appl. Phys. 81 (1997) 4125.
[25] D.G. Park, J.H. Hong, K.S. Jang, M.M. Jung, G.M. Kim, J. Kor. Phys. Soc. 34 (1999) 434.
[26] K.O. Chang, S.H. Chi, K.J. Choi, B.C. Kim, S.L. Lee, Int. J. Pres. Ves. Pip. 79 (2002) 753.
[27] P. Asoka-Kumar, B.D. Wirth, P.A. Sterne, R.H. Howell, G.R. Odette, Philos. Mag. Lett. 82 (2002) 609.
[28] M.K. Miller, B.D. Wirth, G.R. Odette, Mater. Sci. Eng. A 353 (2003) 133.
[29] S.C. Glade, B.D. Wirth, G.R. Odette, P. Asoka-Kumar, P.A. Sterne, R.H. Howell, Philos. Mag. 85 (2005) 629.
[30] C.P. Steinmetz, Trans. Am. Inst. Electr. Eng. 9 (1892) 3.
[31] A. Okada, N. Kawaguchi, M.L. Hamilton, K. Hamada, T. Yoshiie, I. Ishida, E. Hirota, J. Nucl. Mater. 212–215 (1994) 382.
[32] M.K. Miller, K.F. Russell, M.A. Sokolov, R.K. Nanstad, J. Nucl. Mater. 361 (2007) 248.
[33] M.K. Miller, K.F. Russell, J. Nucl. Mater. 371 (2007) 145.
[34] I.M. Robertson, M.L. Jenkins, C.A. English, J. Nucl. Mater. 108–109 (1982) 209.
[35] L.L. Horton, J. Bentley, K. Farrell, J. Nucl. Mater. 108–109 (1982) 222.
[36] J. Kočík, E. Keilová, J. Čížek, I. Procházka, J. Nucl. Mater. 303 (2002) 52.